

2021

Fifteen Years of HFC-134a Satellite Observations: Comparisons with SLIMCAT Calculations

Jeremy J. Harrison

Martyn P. Chipperfield


Christopher D. Boone

Sandip S. Dhomse

Peter F. Bernath

Old Dominion University, pbernath@odu.edu

Follow this and additional works at: https://digitalcommons.odu.edu/chemistry_fac_pubs

 Part of the [Atmospheric Sciences Commons](#), [Climate Commons](#), and the [Environmental Chemistry Commons](#)

Original Publication Citation

Harrison, J. J., Chipperfield, M. P., Boone, C. D., Dhomse, S. S., & Bernath, P. F. (2021). Fifteen years of HFC-134a satellite observations: Comparisons with SLIMCAT calculations. *Journal of Geophysical Research: Atmospheres*, 126(8), 1-11, Article e2020JD033208. <https://doi.org/10.1029/2020JD033208>

This Article is brought to you for free and open access by the Chemistry & Biochemistry at ODU Digital Commons. It has been accepted for inclusion in Chemistry & Biochemistry Faculty Publications by an authorized administrator of ODU Digital Commons. For more information, please contact digitalcommons@odu.edu.



RESEARCH ARTICLE

10.1029/2020JD033208

Key Points:

- First comparison between long-term satellite measurements (ACE-FTS) of atmospheric HFC-134a and a 3D chemical transport model (SLIMCAT)
- Observations agree well with SLIMCAT, although ACE-FTS is biased low by up to 10–15 ppt in the troposphere between 30°S and 30°N
- Global trends are linear to a good approximation: 4.49 ppt/year for ACE-FTS (2004–2018; 5.5–24.5 km) and 4.66 ppt/year for SLIMCAT

Correspondence to:

J. J. Harrison,
jh592@leicester.ac.uk

Citation:

Harrison, J. J., Chipperfield, M. P., Boone, C. D., Dhomse, S. S., & Bernath, P. F. (2021). Fifteen years of HFC-134a satellite observations: Comparisons with SLIMCAT calculations. *Journal of Geophysical Research: Atmospheres*, 126, e2020JD033208. <https://doi.org/10.1029/2020JD033208>

Received 1 JUN 2020

Accepted 17 FEB 2021

Author Contributions:

Conceptualization: Jeremy J. Harrison, Martyn P. Chipperfield
Data curation: Christopher D. Boone, Peter F. Bernath
Formal analysis: Jeremy J. Harrison
Software: Martyn P. Chipperfield, Sandip S. Dhomse
Visualization: Jeremy J. Harrison
Writing – original draft: Jeremy J. Harrison
Writing – review & editing: Christopher D. Boone, Sandip S. Dhomse, Peter F. Bernath

Fifteen Years of HFC-134a Satellite Observations: Comparisons With SLIMCAT Calculations

Jeremy J. Harrison^{1,2} , Martyn P. Chipperfield^{3,4} , Christopher D. Boone⁵ , Sandip S. Dhomse^{3,4} , and Peter F. Bernath^{5,6}

¹Department of Physics and Astronomy, University of Leicester, Leicester, UK, ²National Centre for Earth Observation, University of Leicester, Leicester, UK, ³Institute for Climate and Atmospheric Science, School of Earth and Environment, University of Leeds, Leeds, UK, ⁴National Centre for Earth Observation, University of Leeds, Leeds, UK, ⁵Department of Chemistry, University of Waterloo, Waterloo, ON, Canada, ⁶Department of Chemistry and Biochemistry, Old Dominion University, Norfolk, VA, USA

Abstract The phase out of anthropogenic ozone-depleting substances such as chlorofluorocarbons under the terms of the Montreal Protocol led to the development and worldwide use of hydrofluorocarbons (HFCs) in refrigeration, air conditioning, and as blowing agents and propellants. Consequently, over recent years, the atmospheric abundances of HFCs have dramatically increased. HFCs are powerful greenhouse gases and are now controlled under the terms of the 2016 Kigali Amendment to the Montreal Protocol. HFC-134a is currently the most abundant HFC in the atmosphere, breaking the 100 ppt barrier in 2018, and can be measured in the Earth's atmosphere by the satellite remote-sensing instrument ACE-FTS (Atmospheric Chemistry Experiment-Fourier Transform Spectrometer), which has been measuring since 2004. This work uses the ACE-FTS v4.0 data product to investigate global distributions and trends of HFC-134a. These measurements are compared with a simulation of SLIMCAT, a state-of-the-art three-dimensional chemical transport model, which is constrained by global surface HFC-134a measurements. The agreement between observation and model is good, although in the tropical troposphere ACE-FTS measurements are biased low by up to 10–15 ppt. The overall ACE-FTS global trend of HFC-134a for the altitude range 5.5–24.5 km and 2004–2018 time period is approximately linear with a value of 4.49 ± 0.02 ppt/year, slightly lower than the corresponding SLIMCAT trend of 4.66 ppt/year. Using a simple box model, we also estimate the annual global emissions and burdens of HFC-134a from the model data, indicating that emissions of HFC-134a have increased almost linearly, reaching 236 Gg by 2018.

1. Introduction

Humanity's love affair with chlorofluorocarbons (CFCs), which began in the middle of the 20th century, was always destined to end in tears. The long, multidecadal atmospheric lifetimes of these chlorine-containing molecules, allowing them to reach the stratosphere, subsequently photodissociate and liberate chlorine atoms, led directly to the depletion of ozone and a thinning of the ozone layer (WMO/UNEP, 2018). Environmental catastrophe, however, was avoided by the ratification of the 1987 Montreal Protocol, which (through later amendments) enacted the phase out of the major ozone-depleting substances (ODSs) such as CFCs and their temporary replacements, hydrochlorofluorocarbons (HCFCs); the latter with smaller ozone-depleting potentials (ODPs) and shorter atmospheric lifetimes than CFCs. One of the most successful environmental treaties ever signed (McKenzie et al., 2019), the Montreal Protocol has reduced the emissions of these ODSs under a legal framework, thereby saving millions of people from the ravages of skin cancer (Chipperfield et al., 2015), although it will be many years before ozone levels recover to previous levels on account of the long atmospheric lifetimes of ODSs, for example, CFC-12 has an overall atmospheric lifetime of 102 years (WMO/UNEP, 2018).

With the phase out of CFCs and HCFCs under the terms of the Montreal Protocol, humanity was forced to look elsewhere to satisfy its desire for refrigerants, in particular to the class of molecules known as hydrofluorocarbons (HFCs). Like CFCs and HCFCs, HFCs are very strong greenhouse gases, many times more powerful than carbon dioxide. For example, the 100-year global warming potential of HFC-23 is 12,690 (WMO/UNEP, 2018) compared with a value of 1 for CO₂, indicating that over a 100-year time period, the

© 2021. The Authors.

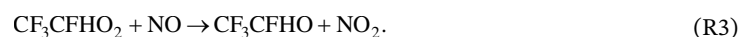
This is an open access article under the terms of the [Creative Commons Attribution License](#), which permits use, distribution and reproduction in any medium, provided the original work is properly cited.

cumulative radiative forcing of climate resulting from the emission of HFC-23 into the atmosphere is 12,690 times greater than for an equivalent unit of CO₂. Although strictly speaking the ODPs of HFCs are zero, as strong radiative forcers they will produce a very small indirect effect on ozone destruction through the increases in tropospheric and stratospheric temperatures, notably by enhancing ozone-destroying catalytic cycles and modifying atmospheric circulation (Hurwitz et al., 2015). Historically, the HFCs have not been regulated by the Montreal Protocol because they do not directly deplete stratospheric ozone. However, the recent Kigali amendment in 2016 has provided a roadmap for their phase out (WMO/UNEP, 2018).

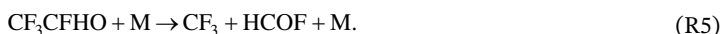
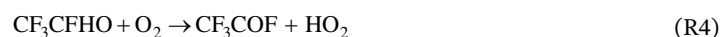
1,1,1,2-Tetrafluoroethane (CF₃CFH₂), or HFC-134a, has replaced CFC-12 as the preferred refrigerant in refrigeration and mobile air conditioning, and is now the most abundant HFC in the atmosphere (WMO/UNEP, 2018). The abundance of HFC-134a has grown steadily since the early 1990s (NOAA, 2018), breaking the 100 ppt barrier in 2018. It has a 100-year global warming potential of 1,360 (WMO/UNEP, 2018), and an atmospheric lifetime of 14 years (WMO/UNEP, 2018). The principal atmospheric sink, accounting for over 99% of the atmospheric degradation of HFC-134a, is the reaction with OH (SPARC, 2013). This proceeds with the breaking of a C-H bond (Kanakidou et al., 1995; Kotamarthi et al., 1998; Wallington et al., 1996)



followed by numerous rapid chemical reactions, of which two of the most important are,



The intermediate CF₃CFHO radicals can either react with O₂ or decompose, according to



It is estimated that 7%–20% of HFC-134a loss proceeds via R4 (Wallington et al., 1996), leading to the formation of CF₃COF; this is removed from the atmosphere (Kotamarthi et al., 1998) to a small extent by surface deposition (2.9%) and photolysis (0.1%), but primarily by hydrolysis (97%) to form trifluoroacetic acid (TFA; CF₃COOH), a persistent, toxic by-product that is removed from the atmosphere by wet deposition and accumulates in oceans, lakes, and other reservoirs. The environmental effects of TFA produced from the degradation of HFCs, HCFCs, and HFOs (hydrofluoroolefins) are currently small, and are expected to remain negligible over the next few decades (WMO/UNEP, 2018). The majority of HFC-134a loss proceeds via R5, where CF₃ leads to the formation of CF₃OH and COF₂. Any HFC-134a reaching the stratosphere will ultimately degrade to the long-lived stratospheric reservoir molecule hydrogen fluoride, HF (Harrison et al., 2016).

The first atmospheric measurements of any HFC from orbit were for HFC-134a (Nassar et al., 2006), taken by the Atmospheric Chemistry Experiment-Fourier transform spectrometer (ACE-FTS). The ACE-FTS, on board SCISAT, has a spectral resolution of 0.02 cm^{−1}, covers the spectral region from 750 to 4,400 cm^{−1}, and currently detects over 40 atmospheric trace gases, more than any other satellite instrument. Having been active since 2004, the ACE-FTS is the only satellite instrument currently able to measure HFCs, including HFC-134a (Nassar et al., 2006) and HFC-23 (Harrison et al., 2012); there is also the potential to retrieve profiles of additional HFCs from the complete period of ACE-FTS observations. With the recent Kigali amendment, monitoring HFC-134a and other HFCs now takes on a greater importance. ACE-FTS measurements provide us with over 15 years of HFC-134a observations with near-global coverage, complementing the existing network of ground-based in situ measurements, and enabling latitudinal and temporal variability to be investigated at elevated altitudes.

The aim of the present work is to understand the HFC-134a global distribution and trends derived from ACE-FTS observations, and use these to validate the HFC-134a mixing ratios output from the SLIMCAT model, a state-of-the-art three-dimensional (3D) chemical transport model (CTM), one of the few to include stratospheric fluorine chemistry. This is the first detailed comparison between satellite observations

of any HFC and a CTM. By extension, we also aim to validate the atmospheric loss processes of HFC-134a in SLIMCAT. The model outputs will then be used to derive tropospheric and stratospheric burdens, annual global emissions of HFC-134a over the observation period, and the annual net fluxes of HFC-134a into the stratosphere.

2. HFC-134a Data Sets

2.1. ACE-FTS

The ACE-FTS instrument uses the sun as a source of infrared radiation for recording limb transmission through the Earth's atmosphere during sunrise and sunset ("solar occultation"). Transmittance spectra are obtained by ratioing against exoatmospheric "high sun" spectra measured each orbit. These spectra, with high signal-to-noise ratios, are recorded through long atmospheric limb paths (~ 300 km effective length), thus providing a low detection threshold for trace species. ACE has an excellent vertical resolution of ~ 3 km and can measure up to 30 occultations per day, with each occultation sampling the atmosphere from 150 km down to the cloud tops (or 5 km in the absence of clouds). The locations of ACE occultations are dictated by the low Earth circular orbit of the spacecraft and the relative position of the sun. Over the course of a year, the ACE-FTS records atmospheric spectra over a large portion of the globe (Bernath et al., 2017), from which it is possible to extract profiles of atmospheric pressure, temperature, and numerous molecules, including many fluorine-containing species.

Although there was no ACE-FTS v3.0/3.5/3.6 HFC-134a data product, an early "research" retrieval based on the v2.2 algorithm has previously been presented using a microwindow over the region $1,180\text{--}1,200\text{ cm}^{-1}$ (ν_5 band) (Nassar et al., 2006). For the present work, the HFC-134a level 2 data set used comes from v4.0 processing of the ACE spectra. Briefly, vertical profiles of trace gases (along with temperature, pressure, and the tangent heights of the measurements) are derived from the recorded transmittance spectra via an iterative Levenberg-Marquardt nonlinear least-squares global fit to the selected spectral region(s) for all measurements within the altitude range of interest. The v4.0 retrieval covers the HFC-134a Q branch of the ν_6 band between 1103.04 and 1105.84 cm^{-1} , for which the spectral residuals are closer to the noise level than for the ν_5 band. All spectroscopic data were taken from the HITRAN 2016 database (Gordon et al., 2017), including the infrared absorption cross sections for HFC-134a, which are described in Harrison (2015). The complete microwindow set, associated altitude ranges, and the spectrally interfering species included in the fit are all defined in Fernando et al. (2019), which describes a preliminary "hybrid" HFC-134a research product specifically created to provide inputs for the 2018 WMO ozone assessment (WMO/UNEP, 2018). This preliminary product was created prior to ACE-FTS v4.0 data processing (Boone et al., 2020), making use of an early version of the v4.0 processing software, with inputs of pressure, temperature, and measurement tangent heights taken from v3.5/v3.6 processing (Boone et al., 2013). Overall, v4.0 confers a number of advantages over previous processing versions, namely substantially more occultations are successfully passed through the processing chain, the instrumental lineshape (ILS) function is better determined, the pointing below 18 km is greatly improved due to the use of the N_2 -collision-induced absorption continuum (Boone & Bernath, 2019), and the temperature and pressure above 18 km are improved by the use of an a priori CO_2 VMR profile varying with time, location, season, and altitude (Toon & Wunch, 2017). The Fernando et al. (2019) study is based on v3.5/v3.6 pressure and temperature retrievals, which use an a priori CO_2 VMR profile that biases derived trends by on average $\sim 0.16\%$ /year (Boone et al., 2020). V4.0 resolves this bias and is therefore more robust for trend analysis.

2.2. TOMCAT/SLIMCAT 3D Chemical Transport Model

The stratospheric configuration of TOMCAT/SLIMCAT (hereafter SLIMCAT), an off-line 3D CTM, calculates the abundances of a number of stratospheric trace gases from prescribed source-gas surface boundary conditions and a detailed treatment of stratospheric chemistry, including the major species in the O_x , NO_y , HO_x , F_y , Cl_y , and Br_y chemical families (e.g., Chipperfield, 1999; Chipperfield et al., 2015; Feng et al., 2007), with the troposphere assumed to be well-mixed. The surface VMRs are specified using data sets prepared for the WMO/UNEP (2018) ozone assessment, and define the long-term tropospheric source gas trends in the model. European Centre for Medium-Range Weather Forecasts (ECMWF) reanalyzes (ERA-Interim

from 1979 onwards) are used to specify winds and temperatures, an approach which gives a realistic stratospheric circulation (Chipperfield, 2006; Monge-Sanz et al., 2007). For this study, SLIMCAT was integrated from 1977 to 2018 at a horizontal resolution of $2.8^\circ \times 2.8^\circ$ (T42 Gaussian grid) and 32 levels from the surface to 60 km. The model initialization used the estimated halocarbon loading for 1977, taken from the WMO/UNEP scenarios. Surface VMRs for HFC-134a were taken from measured global annual mean dry-air mole fractions used in deriving the radiative forcing values provided in the NOAA Annual Greenhouse Gas Index (AGGI) (NOAA, 2018). As outlined in Harrison et al. (2016), the atmospheric degradation chemistry scheme for HFC-134a in SLIMCAT is somewhat crude, simply assuming one CH_2FCF_3 molecule directly leads to the formation of one COF_2 molecule and two HF molecules. However, this is not a problem for direct comparisons of source gas calculations with observations because there is essentially only one sink (reaction with OH) and no additional sources other than emissions at the surface.

3. Comparison Between ACE-FTS/SLIMCAT HFC-134a Data Sets

Prior to analysis, ACE-FTS data were filtered in order to remove significant outliers. The HFC-134a data at each altitude were temporally and spatially binned into 30 half-year periods (defined as January-June and July-December, from 2004 to 2018) and 20° latitude bands. Within each bin, those data outside two median absolute deviations of the median mixing ratio were removed. The 1σ statistical fitting errors for a single HFC-134a profile are typically 50–80 ppt in the tropical lower troposphere (as low as 5.5 km), and 20–60 ppt in the rest of the atmosphere (as high as 24.5 km). These errors are random in nature and largely determined by the measurement noise of the ACE-FTS instrument and the strength of the absorption signal for the molecular feature of interest. As such, it is a very difficult task to successfully optimize a microwindow with 1σ statistical fitting errors of this magnitude. It is only after averaging multiple profiles that these random errors reduce (by a factor of $1/\sqrt{N}$, where N is the number of profiles), and systematic errors reveal themselves; these systematic errors can arise from uncertainties in temperature, pressure, tangent altitude (i.e., pointing) instrumental line shape (ILS), and the spectroscopic data of absorbing species in the microwindow.

The upper panel of Figure 1 shows ACE-FTS HFC-134a means on a 1-km altitude grid for all filtered 2018 data within 10° latitude bins. The lower panels show the corresponding SLIMCAT means for 2018, sampled in two different ways; first at the ACE-FTS measurement locations and averaged within the same 10° latitude bins, and second as full zonal means (integrated over all longitudes) on the model 2.8° grid but interpolated to the center of the ACE-FTS latitude bins. The two SLIMCAT plots provide a measure of how the irregular ACE-sampling affects the observed zonal means; in this case, the largest differences occur at the southern high latitudes. Figure 2 provides a complementary perspective, showing mean ACE-FTS profiles in 20° latitude bands over three years: 2006, 2012, 2018 with superimposed error bars representing one mean absolute deviation from the bin mean, and mean SLIMCAT profiles once again sampled at the ACE-FTS measurement locations. The vertical resolution of the SLIMCAT profiles, $\sim 1\text{--}2$ km, is higher than for the ACE-FTS (~ 3 km). The ACE-FTS retrieval scheme does not utilize the optimal estimation method, so there are no averaging kernels to apply to the model profiles. Therefore, as the difference in vertical resolution is not too large, we do not explicitly account for this in the comparisons. On the whole the agreement between observations and model is good; however, there are some substantial differences, notably the large negative bias of up to 10–15 ppt in the tropical troposphere, and a slightly larger negative bias at the top of the retrieval range. As the troposphere is well-mixed and the retrieved tropospheric ACE-FTS VMRs are lower than the surface values used to constrain the model calculations, the discrepancy is likely due to retrieval errors arising from inadequacies in the spectroscopy of interfering species within the microwindow, most likely due to water vapor. The ACE-FTS data indicate slightly higher tropospheric VMRs in the Northern Hemisphere, where higher emissions are expected, however quantifying this hemispheric difference is particularly challenging due to the aforementioned bias. The annual mean dry-air mole fractions used to force SLIMCAT are global with no latitude dependence, so the model implicitly assumes there is no hemispheric difference in emissions.

The bias at the top of the retrieval range is likely a retrieval artifact, with two possible explanations. The first is that the microwindow suffers from ozone interference (the top of the retrieval range is located near

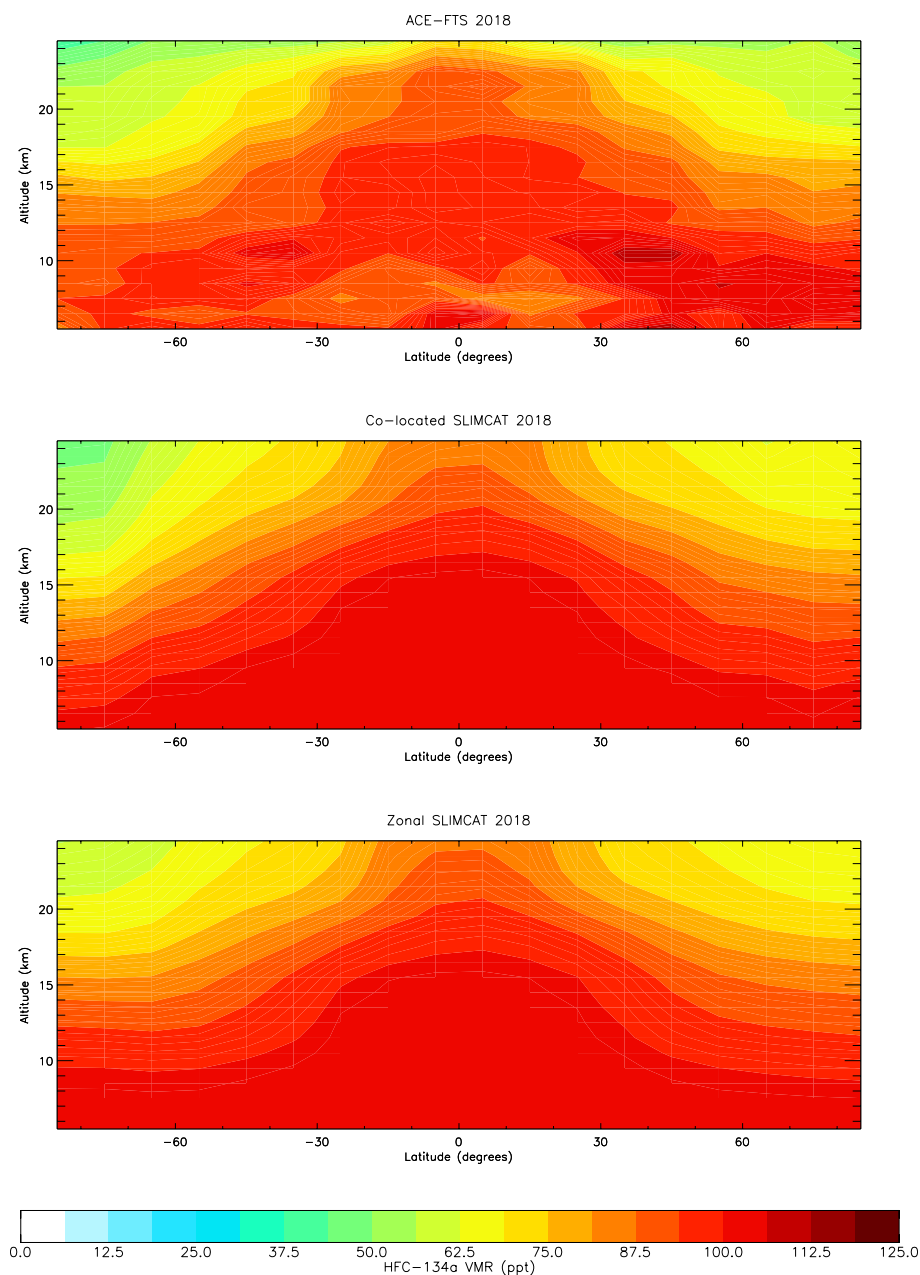


Figure 1. Top: ACE-FTS zonal means of HFC-134a calculated on the standard 1-km-interpolated altitude grid within 10° latitude bins for all filtered ACE-FTS data measured during 2018. Middle: SLIMCAT means, sampled at the actual ACE-FTS measurement locations for 2018 and averaged within 10° latitude bins. Bottom: 2018 SLIMCAT zonal means sampled uniformly in space, and interpolated from the model 2.8° grid to the center of each of the 10° ACE-FTS latitude bins. ACE-FTS, Atmospheric Chemistry Experiment-Fourier Transform Spectrometer.

where the ozone layer peaks), and small spectroscopic residuals associated with ozone lines, which arise from limitations of the underlying HITRAN spectroscopy, will cause systematic errors in the retrieved HFC-134a VMRs. The second possible explanation is more subtle. For the highest analyzed measurement, that is, just below 25 km, the retrieved VMR in the tangent layer relies to a certain extent on the scaling of an “initial” VMR profile, needed to approximate the VMRs in the higher layers where HFC-134a spectroscopic signal is generally below the noise level. Although HFC-134a is not retrieved above 25 km, the calculated spectrum is still generated from the sum of contributions from the tangent layer up to 150 km. The scaling factor is determined during the retrieval by forcing the calculated spectrum to match as best as possible the

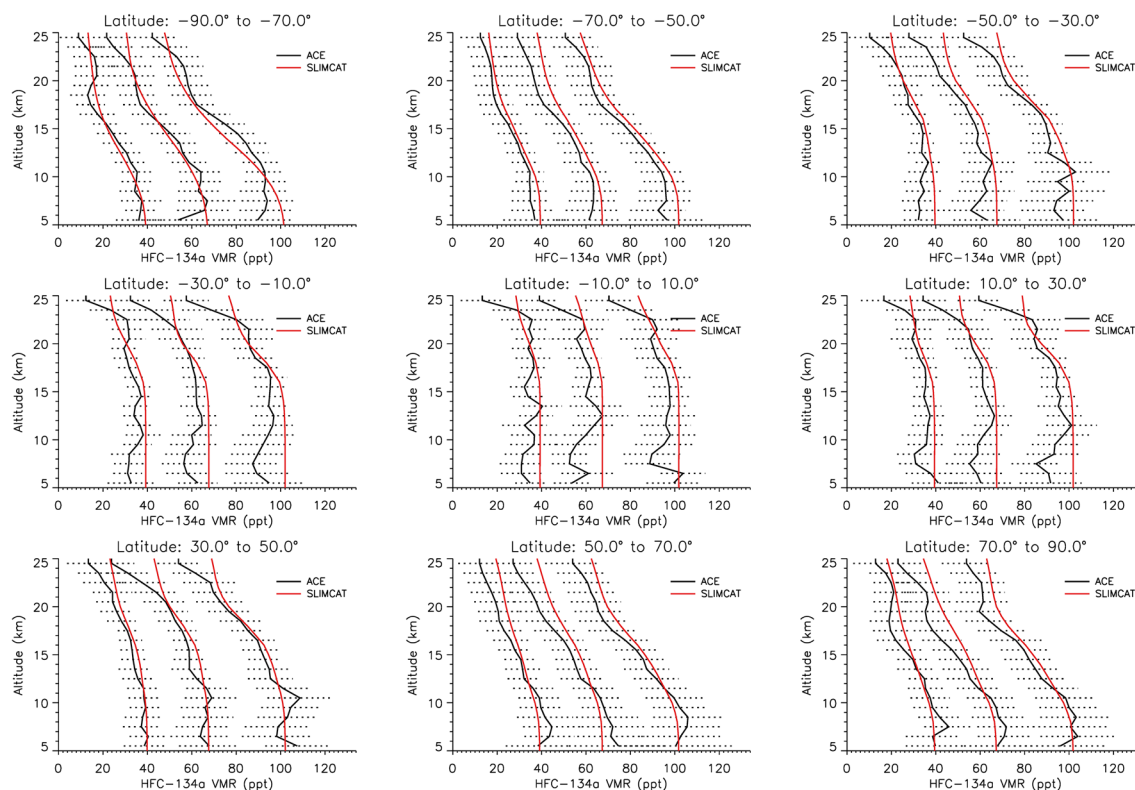


Figure 2. Mean ACE-FTS profiles of HFC-134a in 20° latitude bands for the years 2006, 2012, and 2018, with superimposed error bars representing one mean absolute deviation of the data; corresponding SLIMCAT profiles (sampled at the ACE-FTS measurement locations) are overplotted. ACE-FTS, Atmospheric Chemistry Experiment-Fourier Transform Spectrometer.

measured spectrum for the highest analyzed measurement. If this profile does not match the natural variability of the atmosphere in the higher layers, it will introduce systematic errors into the highest altitudes of the retrieved profile.

4. Trends in Atmospheric HFC-134a

With emissions continuing around the world, atmospheric concentrations of HFC-134a continue to increase rapidly. In this section, trends in the ACE-FTS and SLIMCAT time series (2004–2018) are quantified as a function of altitude (on the ACE-FTS grid) and latitude (in 10° bins) using a simple linear regression model. Due to the ACE-FTS sampling, some latitude bins have fewer points in the regression, particularly in the tropical region. The trend analysis uses SLIMCAT means both derived from calculations sampled at the ACE-FTS measurement locations, and from uniform, zonal sampling for each latitude bin and month. This way, one can estimate whether the ACE-FTS nonuniform sampling creates any significant bias in the trends.

Figure 3 shows ACE-FTS time series plots at 10.5-km altitude between 50°S and 40°N; over plotted are the corresponding colocated SLIMCAT time series, along with the surface annual mean dry-air mole fractions (NOAA, 2018) used to force the model. Due to the long tropospheric lifetime, HFC-134a is well-mixed in the troposphere and there is very little difference between time series at the surface and model at 10.5 km (which lies within the troposphere). Figure 4 presents these trends in the growth of HFC-134a (ppt/year) (January 2004 to December 2018) for ACE and SLIMCAT as a contour plot for the altitude range 5.5–24.5 km; there are two SLIMCAT plots, the first using colocated SLIMCAT data, and the second using uniform zonal mean data. As with the mixing ratios themselves, biases in the trends are apparent; notably the observed trends are lower than the model trends within the tropopause and at the top of the altitude range. Fernando

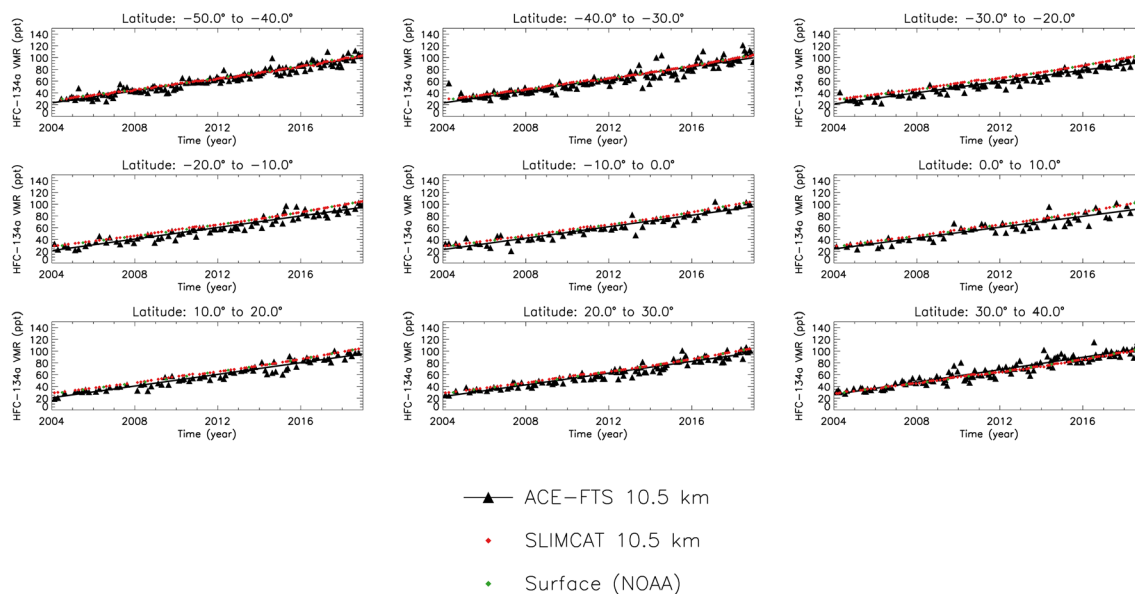


Figure 3. ACE-FTS time series plots of HFC-134a at 10.5-km altitude for 10° latitude bins between 50°S and 40°N (black triangles); over plotted are the corresponding colocated SLIMCAT time series (red triangles). In black are lines of best fit for each ACE-FTS time series. ACE-FTS, Atmospheric Chemistry Experiment-Fourier Transform Spectrometer.

et al. (2019) have previously established the consistency between ACE-FTS trends and those at the surface; the present work confirms this.

The overall global trend of ACE-FTS HFC-134a for the altitude range 5.5–24.5 km, weighted by the cosine of the central latitude for each bin, is 4.49 ± 0.02 ppt/year. This is slightly lower than the global linear trend of 4.9 ± 0.1 ppt/year derived from the preliminary “hybrid” v3.5/v3.6/v4.0 ACE-FTS HFC-134a re-search product, calculated from unweighted annual averages of all data between 6.5 and 15.5 km (Fernando et al., 2019) over the slightly shorter period January 2004 to February 2018. For the latter case, the exclusion of data above 16 km, where trends are lower, is a significant reason for this discrepancy; recalculating the global v4.0 trend over the 6.5–15.5-km altitude range gives a value of 4.79 ± 0.03 ppt/year. Note also that the trend in the surface data taken from the NOAA AGGI is 5.10 ppt/year. Weighted trends for both the zonal mean and ACE-colocated SLIMCAT data are 4.68 and 4.66 ppt/year, respectively. This very small difference ($\sim 0.4\%$) indicates that for HFC-134a, the nonuniform ACE-FTS sampling has no significant effect on the calculation of global trends. However, the SLIMCAT plots in Figure 4 do point to minor differences in the altitude-latitude trends, particularly near the poles; note, for example, the -85°N -centered bin for which the trends in the colocated plot decrease more rapidly with increasing altitude. The low bias in the global ACE-FTS trend of 4.49 ± 0.02 ppt/year relative to the comparable SLIMCAT trend of 4.66 ppt/year is largely due to the low biases of the ACE-FTS VMRs in the troposphere and at the top of the retrieval range.

5. Emissions of Atmospheric HFC-134a

Having validated the SLIMCAT HFC-134a calculations, despite the few regions of bias in the ACE-FTS data, these model outputs are now used to estimate the global emissions of HFC-134a and its partitioning between the troposphere and stratosphere. In order to separate out the tropospheric and stratospheric HFC-134a burdens, we define a climatological tropopause (Lawrence et al., 2001) as

$$p = 300 - 215 \cos^2(\varphi), \quad (1)$$

where p is the pressure in hPa and φ is the latitude. Time series of the modeled HFC-134a burdens are shown in Figure 5a. The ratio of the HFC-134a burden between the troposphere and stratosphere only

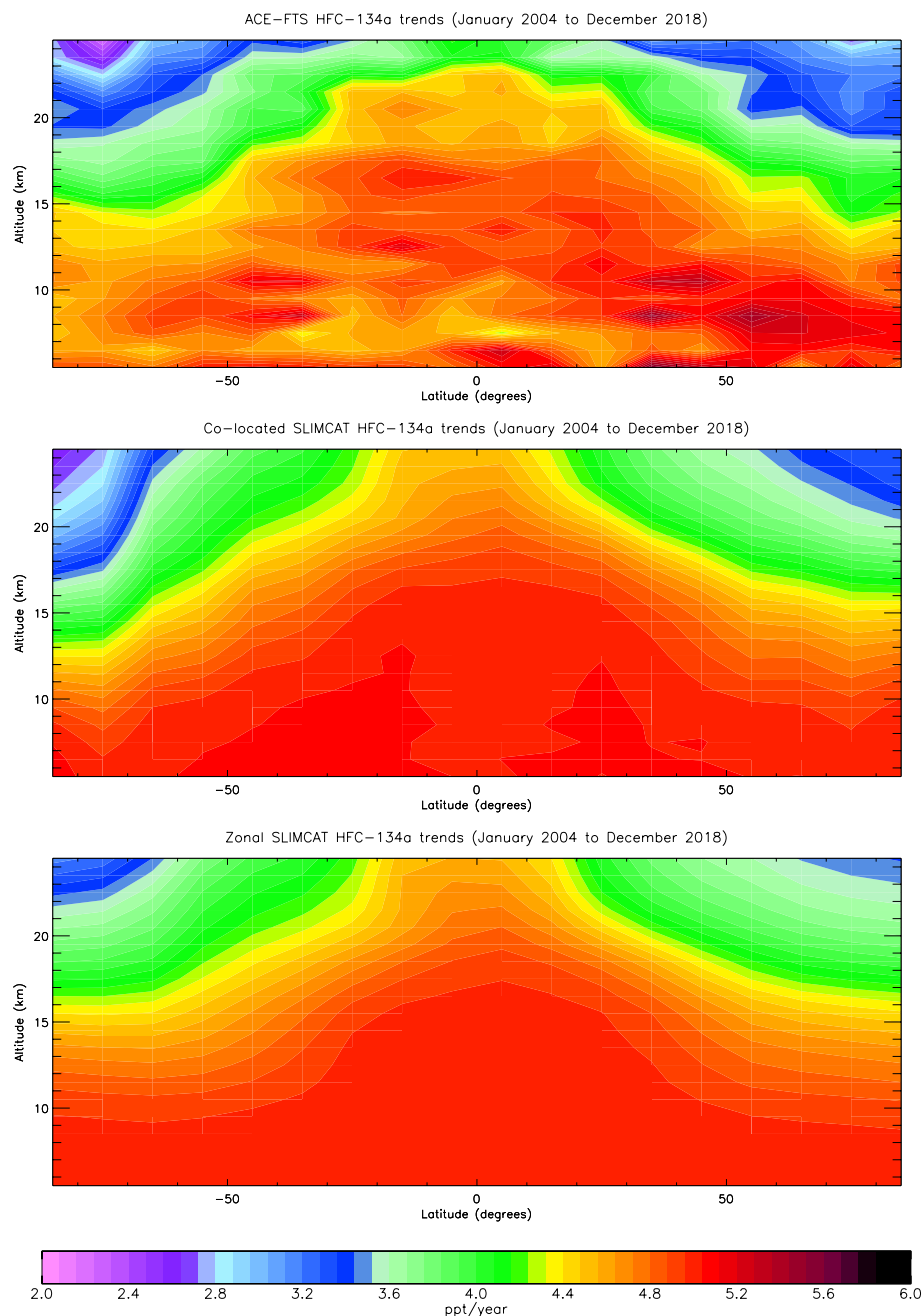


Figure 4. Trends in the growth of HFC-134a (ppt/year; January 2004 to December 2018) for ACE-FTS and SLIMCAT as a function of latitude and altitude; there are two SLIMCAT plots, the first using SLIMCAT data colocated at the ACE-FTS measurement locations and averaged within 10° latitude bins, the second using SLIMCAT data sampled uniformly in space and interpolated to the center of each of the 10° ACE-FTS latitude bins. A full discussion of these trends is provided in the text. ACE-FTS, Atmospheric Chemistry Experiment-Fourier Transform Spectrometer.

changes little over the observation period; by December 2018 12.1% of the total atmospheric HFC-134a, equivalent to 201.7 Gg (or 150.2 Gg of fluorine), resides in the stratosphere. Assuming steady state conditions and values of 15.3, 267, and 14.4 years for the tropospheric, stratospheric, and total lifetimes, respectively, (refer to Table 5.6 of SPARC, 2013), 5.4% of the total loss occurs in the stratosphere, the remainder in the troposphere. The much longer lifetime of HFC-134a in the stratosphere means that the relative destruction there is less than half of the relative burden; there is significant recirculation of the HFC back to the troposphere where it is mainly destroyed.

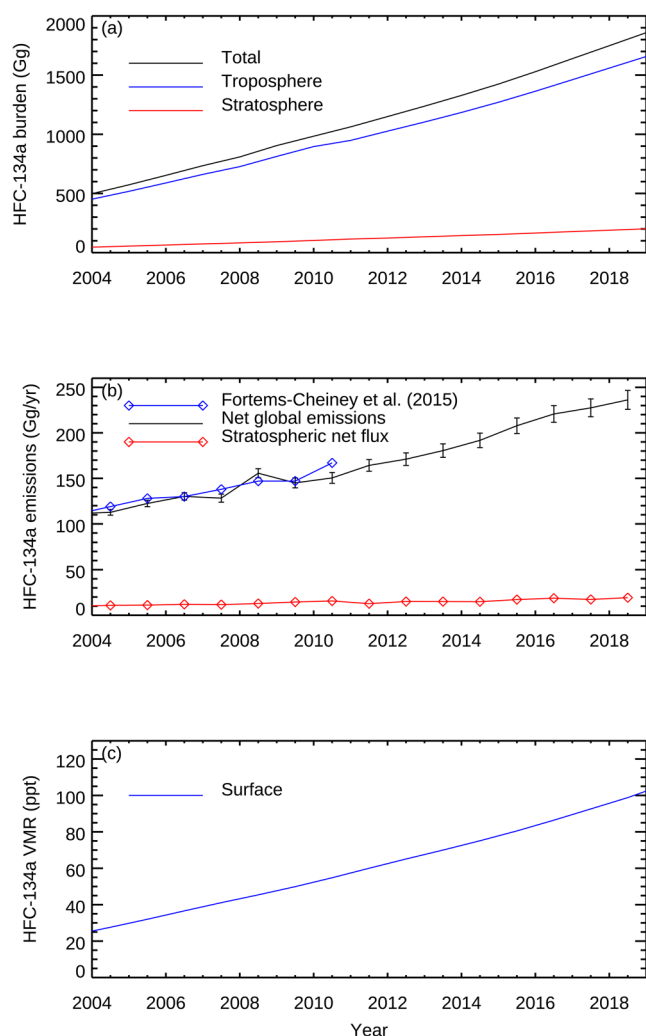


Figure 5. (a) The time series of HFC-134a total atmospheric, tropospheric, and stratospheric burdens (Gg) determined from SLIMCAT. The tropopause is defined by Equation 1. (b) The time series of annual global emissions of HFC-134a (Gg/yr) determined from a global box model using atmospheric burdens from SLIMCAT as input. Error bars correspond to the calculated annual global emissions for a 9% (1σ) change in the HFC-134a total atmospheric lifetime. Overplotted are global emissions from Fortems-Cheiney et al. (2015). Also shown is the estimated annual net flux of HFC-134a into the stratosphere based on the chemical loss in that region. (c) Global mean surface HFC-134a VMRs used in SLIMCAT which are taken from measured global annual mean dry-air mole fractions provided in the NOAA AGGI (NOAA, 2018).

A simple global box model previously used to study CH_4 , CH_3CCl_3 (McNorton et al., 2016), and CH_2Cl_2 (Hossaini et al., 2017) emissions has been used to derive the global annual HFC-134a emissions required to sustain the modeled burdens. Using the SPARC total lifetime for HFC-134a, the box model indicates annual global emissions have more than doubled between 2004 and 2018, from 113 to 236 Gg. Figure 5b displays the time series of these derived annual global emissions, which compare well with global emissions derived by Fortems-Cheiney et al. (2015) up to 2010 from inversions of a wide range of global surface measurements. Our results therefore extend this time series and show almost linearly increasing emissions through 2018. In a similar manner, we also estimate the net flux of HFC-134a into the stratosphere; Figure 5b displays the time series of these derived annual stratospheric fluxes. By extrapolating the modeled atmospheric burdens back to the early 1990s with the aid of the NOAA AGGI data, and using the stratospheric lifetime of 267 years, we estimate that ~ 70 Gg of HFC-134a in total has degraded in the stratosphere by the end of 2018.

Calculating stratospheric fluxes and burdens from model output depends explicitly on the choice of the tropopause. Here, we use a climatological tropopause (see Equation 1), but other definitions could be used, for example, a chemical tropopause corresponding to 150 ppbv O_3 . Sensitivity tests show that such a tropopause would introduce seasonality into the analysis and increase the derived stratospheric masses by on average $\sim 13\%$.

6. Conclusions

With the announcement of a global phase out of HFCs under the terms of the recent Kigali Amendment to the Montreal Protocol, the monitoring of their atmospheric abundances now takes on a greater importance. This work has investigated global distributions and trends of HFC-134a, the most abundant HFC in the atmosphere, from 15 years of measurements by the ACE-FTS instrument, which has been recording atmospheric spectra since 2004. Currently the ACE-FTS is the only satellite instrument making measurements of HFCs from orbit.

The ACE-FTS measurements are compared with the output of SLIMCAT, a state-of-the-art 3D CTM constrained by observed surface mixing ratios. In general, the agreement is good, although in the troposphere between 30°S and 30°N the ACE-FTS measurements are biased low by as much as 10–15 ppt. This points to the same bias being present between the ACE-FTS and surface in-situ observations. The growth in atmospheric HFC-134a observed by the ACE-FTS is well modeled by a linear term. Over the altitude range 5.5–24.5 km and the time period January 2004 to December 2018, the ACE-FTS growth rate is 4.49 ± 0.02 ppt/year, slightly lower than the corresponding SLIMCAT trend of 4.66 ppt/year; this difference is directly linked with the small tropospheric bias in the ACE-FTS retrieval.

With a simple box model, we have calculated the annual global emissions and burdens of HFC-134a using a climatological definition of the tropopause. Estimated annual global emissions of HFC-134a have increased almost linearly, reaching 236 Gg by 2018. Our results extend previous estimates that only went up to 2010, and show that emissions of HFC-134a have continued to grow through 2018.

Data Availability Statement

ACE-FTS data were obtained from https://database.scisat.ca/level2/ace_v4.0/. The SLIMCAT model data are available at <http://doi.org/10.5281/zenodo.4596550>

Acknowledgments

This study was funded as part of the UK Research and Innovation Natural Environment Research Council's support of the National Centre for Earth Observation, contract number PR140015. The ACE satellite mission is funded primarily by the Canadian Space Agency (CSA). M. P. Chipperfield and S. S. Dhomse thank Wuhu Feng (the National Centre for Atmospheric Science; NCAS) for help with SLIMCAT. M. P. Chipperfield is a Royal Society Wolfson Research Merit Award holder. We thank the ECMWF for providing the ERA-Interim reanalyses and NOAA for providing the AGGI surface annual mean dry-air mole fractions used by the SLIMCAT model.

References

- Bernath, P. F. (2017). The atmospheric chemistry experiment (ACE). *Journal of Quantitative Spectroscopy and Radiative Transfer*, 186, 3–16. <https://doi.org/10.1016/j.jqsrt.2016.04.006>
- Boone, C. D., & Bernath, P. F. (2019). Tangent height determination from the N₂-continuum for the atmospheric chemistry experiment Fourier transform spectrometer. *Journal of Quantitative Spectroscopy and Radiative Transfer*, 238, 106481. <https://doi.org/10.1016/j.jqsrt.2019.04.033>
- Boone, C. D., Bernath, P. F., Cok, D., Jones, S. C., & Steffen, J. (2020). Version 4 retrievals for the atmospheric chemistry experiment Fourier transform spectrometer (ACE-FTS) and imagers. *Journal of Quantitative Spectroscopy and Radiative Transfer*, 247, 106939. <https://doi.org/10.1016/j.jqsrt.2020.106939>
- Boone, C. D., Walker, K. A., & Bernath, P. F. (2013). Version 3 retrievals for the Atmospheric Chemistry Experiment Fourier Transform Spectrometer (ACE-FTS). In P. F. Bernath (Ed.), *The atmospheric chemistry experiment ACE at 10: A solar occultation anthology* (pp. 103–127). Hampton, VA: A. Deepak Publishing. Retrieved from <http://www.ace.uwaterloo.ca/publications/2013/Version3.5retrievals2013.pdf>
- Chipperfield, M. P. (1999). Multiannual simulations with a three-dimensional chemical transport model. *Journal of Geophysical Research*, 104, 1781–1805. <https://doi.org/10.1029/98JD02597>
- Chipperfield, M. P. (2006). New version of the TOMCAT/SLIMCAT off-line chemical transport model: Intercomparison of stratospheric tracer experiments. *Quarterly Journal of the Royal Meteorological Society*, 132, 1179–1203. <https://doi.org/10.1256/qj.05.51>
- Chipperfield, M. P., Dhomse, S. S., Feng, W., McKenzie, R. L., Velders, G. J. M., & Pyle, J. A. (2015). Quantifying the ozone and ultraviolet benefits already achieved by the Montreal Protocol. *Nature Communications*, 6, 7233. <https://doi.org/10.1038/ncomms8233>
- Feng, W., Chipperfield, M. P., Dorf, M., Pfeilsticker, K., & Ricaud, P. (2007). Mid-latitude ozone changes: Studies with a 3-D CTM forced by ERA-40 analyses. *Atmospheric Chemistry and Physics*, 7, 2357–2369. <https://doi.org/10.5194/acp-7-2357-2007>
- Fernando, A. M., Bernath, P. F., & Boone, C. D. (2019). Trends in atmospheric HFC-23 (CHF₃) and HFC-134a abundances. *Journal of Quantitative Spectroscopy and Radiative Transfer*, 238, 106540. <https://doi.org/10.1016/j.jqsrt.2019.06.019>
- Fortems-Cheiney, A., Saunio, M., Pison, I., Chevallier, F., Bousquet, P., Cressot, C., et al. (2015). Increase in HFC-134a emissions in response to the success of the Montreal Protocol. *Journal of Geophysical Research: Atmospheres*, 120, 11728–11742. <https://doi.org/10.1002/2015JD023741>
- Gordon, I. E., Rothman, L. S., Hill, C., Kochanov, R. V., Tan, Y., Bernath, P. F., et al. (2017). The HITRAN2016 molecular spectroscopic database. *Journal of Quantitative Spectroscopy and Radiative Transfer*, 203, 3–69. <https://doi.org/10.1016/j.jqsrt.2017.06.038>
- Harrison, J. J. (2015). Infrared absorption cross sections for 1,1,1,2-tetrafluoroethane. *Journal of Quantitative Spectroscopy and Radiative Transfer*, 151, 210–216. <https://doi.org/10.1016/j.jqsrt.2014.09.023>
- Harrison, J. J., Boone, C. D., Brown, A. T., Allen, N. D. C., Toon, G. C., & Bernath, P. F. (2012). First remote sensing observations of trifluoromethane (HFC-23) in the upper troposphere and lower stratosphere. *Journal of Geophysical Research*, 117, D05308. <https://doi.org/10.1029/2011JD016423>
- Harrison, J. J., Chipperfield, M. P., Boone, C. D., Dhomse, S. S., Bernath, P. F., Froidevaux, L., et al. (2016). Satellite observations of stratospheric hydrogen fluoride and comparisons with SLIMCAT calculations. *Atmospheric Chemistry and Physics*, 16, 10501–10519. <https://doi.org/10.5194/acp-16-10501-2016>
- Hossaini, R., Chipperfield, M. P., Montzka, S. A., Leeson, A. A., Dhomse, S. S., & Pyle, J. A. (2017). The increasing threat to stratospheric ozone from dichloromethane. *Nature Communications*, 8, 15962. <https://doi.org/10.1038/ncomms15962>
- Hurwitz, M. M., Fleming, E. L., Newman, P. A., Li, F., Mlawer, E., Cady-Pereira, K., & Bailey, R. (2015). Ozone depletion by hydrofluorocarbons. *Geophysical Research Letters*, 42, 8686–8692. <https://doi.org/10.1002/2015GL065856>
- Kanakidou, M., Dentener, F. J., & Crutzen, P. J. (1995). A global three-dimensional study of the fate of HCFCs and HFC-134a in the troposphere. *Journal of Geophysical Research*, 100, 18781–18801. <https://doi.org/10.1029/95JD01919>
- Kotamarthi, V. R., Rodriguez, J. M., Ko, M. K. W., Tromp, T. K., Sze, N. D., & Prather, M. J. (1998). Trifluoroacetic acid from degradation of HCFCs and HFCs: A three-dimensional modeling study. *Journal of Geophysical Research*, 103, 5747–5758. <https://doi.org/10.1029/97JD02988>
- Lawrence, M. G., Jöckel, P., & von Kuhlmann, R. (2001). What does the global mean OH concentration tell us? *Atmospheric Chemistry and Physics*, 1, 37–49. <https://doi.org/10.5194/acp-1-37-2001>
- McKenzie, R., Bernhard, G., Liley, B., Disterhoft, P., Rhodes, S., Bais, A., et al. (2019). Success of Montreal Protocol demonstrated by comparing high-quality UV measurements with “World Avoided” calculations from two chemistry-climate models. *Scientific Reports*, 9, 12332. <https://doi.org/10.1038/s41598-019-48625-z>
- McNorton, J., Chipperfield, M. P., Gloor, M., Wilson, C., Feng, W., Hayman, G. D., et al. (2016). Role of OH variability in the stalling of the global atmospheric CH₄ growth rate from 1999 to 2006. *Atmospheric Chemistry and Physics*, 16, 7943–7956. <https://doi.org/10.5194/acp-16-7943-2016>
- Monge-Sanz, B. M., Chipperfield, M. P., Simmons, A. J., & Uppala, S. M. (2007). Mean age of air and transport in a CTM: Comparison of different ECMWF analyses. *Geophysical Research Letters*, 34, L04801. <https://doi.org/10.1029/2006GL028515>
- Nassar, R., Bernath, P. F., Boone, C. D., McLeod, S. D., Skelton, R., Walker, K. A., et al. (2006). A global inventory of stratospheric fluorine in 2004 based on atmospheric chemistry experiment Fourier transform spectrometer (ACE-FTS) measurements. *Journal of Geophysical Research*, 111, D22313. <https://doi.org/10.1029/2006JD007395>
- NOAA. (2018). *Annual greenhouse gas Index (AGGI)*. Retrieved from <https://www.esrl.noaa.gov/gmd/aggi/aggi.html>
- SPARC. (2013). SPARC report on the lifetimes of stratospheric ozone-depleting substances, their replacements, and related species. In M. Ko, P. Newman, S. Reimann, & S. Strahan (Eds.), *SPARC Report No. 6, WCRP-15/2013*.
- Toon, G. C., & Wunch, D. (2017). *A stand-alone a priori profile generation tool for GGG2014 release*. CaltechDATA. <https://doi.org/10.14291/tcon.ggg2014.priors.r0/1221661>

Wallington, T. J., Hurley, M. D., Fracheboud, J. M., Orlando, J. J., Tyndall, G. S., Sehested, J., et al. (1996). Role of excited CF_3CFHO radicals in the atmospheric chemistry of HFC-134a. *Journal of Physical Chemistry A*, *100*, 18116–18122. <https://doi.org/10.1021/jp9624764>

WMO/UNEP. (2018). *Scientific assessment of ozone depletion: 2018* (Global Ozone Research and Monitoring Project-Report No. 58). Geneva, Switzerland.